Relativistic multiconfiguration approach to the spin polarization of slow electrons elastically scattered from krypton

J. E. Sienkiewicz* and W. E. Baylis

Department of Physics, University of Windsor, Windsor, Ontario, Canada N9B 3P4

(Received 6 December 1995; revised manuscript received 25 September 1996)

The elastic scattering of electrons from krypton atoms is calculated in a relativistic multiconfiguration method. The correlation effects responsible for target polarization are treated in a relativistic configuration-interaction scheme that allows for dynamic effects. Calculations of the spin polarization S at 5, 10, 15, and 20 eV are discussed and compared with experimental and other theoretical data. We also show spin-polarization trajectories that represent all three scattering parameters S, T, and U in a single computationally significant curve. [S1050-2947(97)04302-3]

PACS number(s): 34.80.Bm, 31.25.Eb

I. INTRODUCTION

In recent years, the scattering of slow electrons by atoms has been studied extensively by both experimentalists and theoreticians. From the theoretical side, difficulties have arisen from the need for precise calculations of target polarization effects. Several approaches have been used in relativistic calculations, including model polarization [1] and the polarized-orbital approximation, both in the nonrelativistic [2] and relativistic [3] methods. A recent relativistic approach to elastic scattering of electrons from atoms describes polarization by a configuration-interaction (CI) procedure [4]. It builds on the nonrelativistic multiconfiguration approach to elastic scattering by atoms developed by Saha and applied to light rare gases [5–7]. Dynamic distortion effects have also been taken into account by the polarized-orbital method [8,9].

In the present paper we develop further the relativistic version of the multiconfiguration and CI approach [4] to describe the polarization of different target states due to the incoming electron charge through bound relativistic configuration expansions. The polarization is different for different kinetic energies of the scattering electron, and thus dynamic effects are taken into account. The relativistic phase shifts obtained by this method are used to calculate spin-polarization and polarization trajectories of electron scattering by krypton in its ground state at energies of 5, 10, 15, and 20 eV. Comparisons are made with the only existing experimental data of Beerlage *et al.* [10].

Except where otherwise specified, we use atomic units.

II. THEORY

A. Relativistic multiconfiguration approach

We describe the N-electron atomic states by multiconfiguration expansions

$$\Phi_a(N,J_aM_aP_a)=\sum_\mu b_{a\mu}\phi_\mu(N,J_aM_aP_a), \qquad (1)$$

where J_a, M_a, and P_a specify the total angular momentum, magnetic quantum number, and parity of the ath atomic state, respectively. The configuration state functions ϕ_μ are built from four-component Dirac spinors [11]

$$u_{n\kappa m}(\mathbf{r})=\frac{1}{r}\begin{pmatrix} P_{n\kappa}(r)\chi_{\kappa m}(\hat{\mathbf{r}}) \\ iQ_{n\kappa}(r)\chi_{-\kappa m}(\hat{\mathbf{r}}) \end{pmatrix}, \qquad (2)$$

where the spin-angular function is given by

$$\chi_{\kappa m}(\hat{\mathbf{r}})=\sum_{\sigma=\pm 1/2}\left\langle jm\left|l,\frac{1}{2},m-\sigma,\sigma\right.\right\rangle Y_l^{m-\sigma}(\hat{\mathbf{r}})\chi_{1/2}^\sigma.$$

Here, $\langle jm|l,2/2,m-\sigma,\sigma\rangle$ is a Clebsch-Gordan coefficient, $Y_l^{m-\sigma}$ is a spherical harmonic, $\chi_{1/2}^\sigma$ is the spin eigenfunction, $P_{n\kappa}$ and $Q_{n\kappa}$ are the large and small components of the Dirac spinor, respectively, and $\kappa=\pm(j+1/2)$ for $l=j\pm 1/2$ where j is the total angular momentum and l is the orbital quantum number. The $(N+1)$-electron Dirac-Coulomb Hamiltonian is

$$H_{N+1}=\sum_{i=1}^{N+1}\left[c\boldsymbol{\alpha}\cdot\mathbf{p}_i+(\beta-I)c^2-\frac{Z}{r_i}\right]+\sum_{i<j}^{N+1}\frac{1}{r_{ij}}, \qquad (3)$$

where $\boldsymbol{\alpha}$, β are the usual Dirac matrices and I is a 4×4 unit matrix.

We define the $(N+1)$-electron scattering-state wave function Ψ_k as the coupled state of an N-electron atomic wave function $\Phi_i(N,J_aM_aP_a)$ and a scattering-electron wave function $u_{\kappa m}$:

$$\Psi_k(N+1,JMP)=\mathcal{A}\sum_{a=1}^{m_a}c_{ak}\Phi_a(N,J_aM_aP_a)u_{\kappa(a)m(a)}$$

$$+\sum_{j=1}^{m_d}d_{jk}\phi_j(N+1,JMP). \qquad (4)$$

*Permanent address: Katedra Fizyki Teoretycznej i Metod Matematycznych, Politechnika Gdańska, PL 80-952 Gdańsk, Poland.

In this equation, the angular parts of the configuration state functions $\Phi_a(N, J_a M_a P_a)$ and the wave functions $u_{\kappa m}$ for the scattered electron are coupled to form states of total angular momentum J, total magnetic quantum number M, and total parity P. The operator $\mathcal{A}$ antisymmetrizes the scattered-electron coordinate with the N atomic-electron coordinates. The $(N+1)$-electron single-configuration state functions ϕ_j are formed only from bound orbitals, and their role will be discussed below; c_{ak} and d_{jk} are the expansion coefficients. The continuum Dirac spinor is defined as

$$u_{\kappa m}(\mathbf{r}) = \frac{1}{r} \begin{pmatrix} P_\kappa(r) \chi_{\kappa m}(\hat{\mathbf{r}}) \\ i Q_\kappa(r) \chi_{-\kappa m}(\hat{\mathbf{r}}) \end{pmatrix}, \tag{5}$$

where now P_κ and Q_κ refer to continuum orbitals. The continuum orbitals are solutions of

$$\left(\frac{d}{dr} + \frac{\kappa}{r} \right) P_\kappa(r) = \left[2c + \frac{1}{c}[\epsilon - V(r)] \right] Q_\kappa(r) + X_Q(r), \tag{6}$$

$$\left(\frac{d}{dr} - \frac{\kappa}{r} \right) Q_\kappa(r) = -\frac{1}{c}[\epsilon - V(r)] P_\kappa(r) - X_P(r), \tag{7}$$

where c is the speed of light and ϵ is the energy of the scattering electron. The direct $V(r)$ and exchange potentials $X_Q(r)$ and $X_P(r)$ are given by Grant [11]. The above equations are solved by the method of outward integration, and the continuum orbitals are all normalized to the same asymptotic flux.

As discussed by Burke *et al.* [12], in Eq. (4) the sum a ranges over all m_a open channels Φ_a and the continuum spinors $u_{\kappa m}$ are coupled to them. Because bound atomic orbitals are omitted for the scattered electron, this expansion cannot be complete. To compensate, the $(N+1)$-electron states ϕ_j have been added, in which all electrons are bound. Only through such states can the scattering electron interact with the target polarization. This second sum of $(N+1)$-electron bound configurations comprises determinants of atomic orbitals from the N-electron calculation that do not accurately represent the $(N+1)$-electron negative ion. Nevertheless, they add needed flexibility to Ψ_k that helps to account for polarization (electron-correlation) effects. In this *ab initio* approach, contributions of the ''exchange polarization'' [13,14] are also included.

The states $\mathcal{A}\Phi_a(N, J_a M_a P_a) u_{\kappa m}$ and $\phi_j(N+1, J M P)$ form an orthogonal basis set. The coefficients of the scattering-state functions Ψ_k are elements of an eigenvector (c_{ak}, d_{jk}), where k is the eigenvector index. We denote the elastic channel by $a=1$ in Eq. (4). The absorption to inelastic channels is described by coefficients $c_{ak} \neq 0$ with $a > 1$ and by the asymptotic form of the corresponding continuum orbital $u_{\kappa m}$. We look for eigenvectors that make Ψ_k an eigenfunction of H_{N+1} with eigenenergy E.

In the case of elastic scattering, when only one channel $(m_a = 1)$ is open, we obtain the coefficients d_{jk} by solving the system of m_d linear equations [5]

$$\langle \mathcal{A}\Phi_1 u_{\kappa m} | H_{N+1} - E | \phi_{j'} \rangle + \sum_j^{m_d} d_{jk} \langle \phi_j | H_{N+1} - E | \phi_{j'} \rangle = 0, \tag{8}$$

where $j' = 1, \ldots, m_d$ and c_{1k} is assumed to be unity. The solution of Eq. (8) determines new direct and exchange potentials and, thus through Eqs. (6) and (7), an improved continuum scattering orbital. This, in turn, can be used in a new calculation of coefficients d_{jk}. The procedure is iterated to self-consistency (five or six cycles usually suffices).

B. Spin-polarization and polarization trajectories

The two complex scattering amplitudes $f(\vartheta)$ (the direct amplitude) and $g(\vartheta)$ (the ''spin-flip'' amplitude) are defined as

$$f(\vartheta) = \frac{1}{2ik} \sum_l \{ (l+1)[\exp(2i\delta_l^+) - 1]$$
$$+ l[\exp(2i\delta_l^-) - 1] \} P_l(\cos\vartheta), \tag{9}$$

$$g(\vartheta) = \frac{1}{2ik} \sum_l [\exp(2i\delta_l^-) - \exp(2i\delta_l^+)] P_l^1(\cos\vartheta), \tag{10}$$

where ϑ is the scattering angle and $P_l(\cos\vartheta)$ and $P_l^1(\cos\vartheta)$ are the Legendre polynomial and the Legendre associated function, respectively [15]; $\delta_l^\pm$ are the relativistic phase shifts where $+$ refers to the solution with $\kappa = -l-1$ and $-$ to that with $\kappa = l$.

The differential cross section and spin polarization for an unpolarized incident beam are given by [15]

$$\sigma(\vartheta) = |f|^2 + |g|^2 \tag{11}$$

and

$$S(\vartheta) = \frac{i(fg^* - f^*g)}{\sigma(\vartheta)}. \tag{12}$$

Two more spin-polarization parameters can be determined when a change in the polarization of the incident polarized electron beam is observed:

$$T(\vartheta) = \frac{|f|^2 - |g|^2}{\sigma(\vartheta)}, \quad U(\vartheta) = \frac{fg^* + f^*g}{\sigma(\vartheta)}. \tag{13}$$

The relation between the direction of the polarization vector and the ratio f/g of complex scattering amplitudes is that between a point on the unit Poincaré sphere and the complex coordinate [16],

$$x_- = x - iy = f/g, \tag{14}$$

of its stereographic projection on the equatorial plane:

$$U = x\zeta, \tag{15}$$

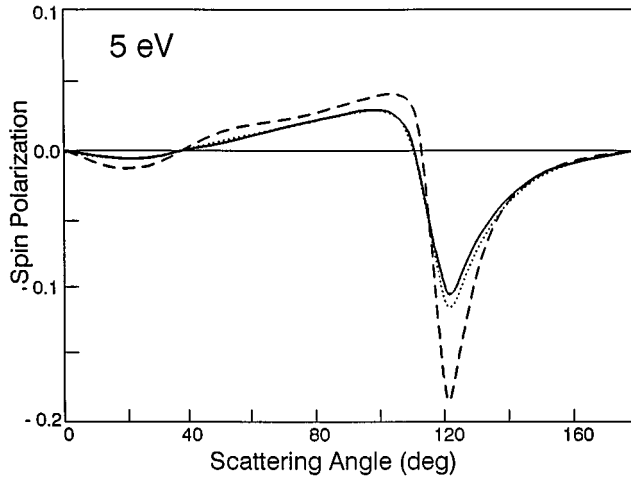$$S = y\zeta, \tag{16}$$

$$T = 1 - \zeta, \tag{17}$$

FIG. 1. Spin polarization as a function of scattering angle at an electron impact energy of 5 eV: solid line, present results; dotted line, present results without target polarization; dashed line, model-polarization potential results of Sienkiewicz and Baylis [23].

$$x_- = (U - iS)/\zeta, \qquad (18)$$

where

$$\zeta := 1 - T = \frac{2}{x^2 + y^2 + 1}.$$

Usually, direct scattering dominates over spin-slip scattering and

$$|f| \gg |g| \Rightarrow (U, S, T) \approx (0, 0, 1). \qquad (19)$$

Polarization structures can occur when $|f|$ drops close to zero, but then $\sigma(\vartheta)$ has a minimum. Small shifts in calculational detail can push the trajectory $x_-(\vartheta)$ through the origin and thereby flip the sign of the structure in S or U. Such flips look important but are, in fact, usually not of much signifi-
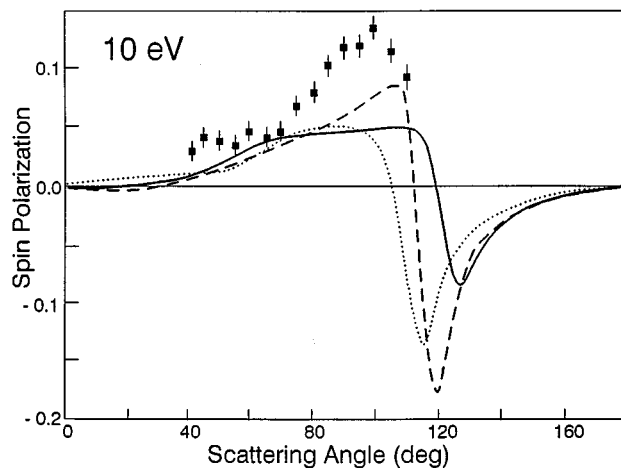
FIG. 2. Spin polarization as a function of scattering angle at an electron impact energy of 10 eV: solid line, present results; dotted line, present results without target polarization; dashed line, model-polarization potential results of Sienkiewicz and Baylis [23]; boxes, experimental results of Beerlage et al. [10].
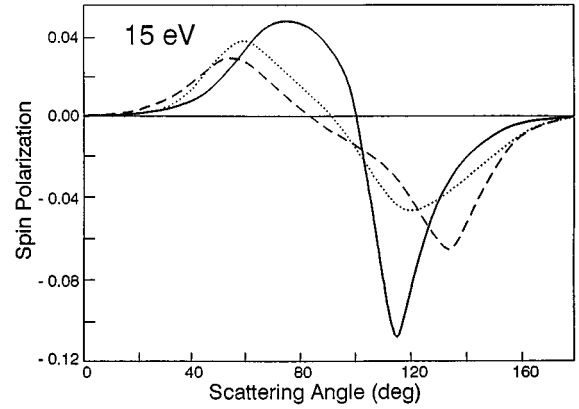
FIG. 3. As in Fig. 1, but at 15 eV.

cance. The trajectories $x_-(\vartheta)$ have more immediate physical significance than the spin parameters U, S, and T.

III. NUMERICAL METHOD

The atomic state wave functions of Eq. (1) are calculated by the relativistic multiconfiguration computer code GRASP2, recently developed by Parpia et al. [17]. This code is the latest published version of the atomic structure package of Grant et al. [18] and Dyall et al. [19]. The atomic orbitals are generated by means of the multiconfiguration self-consistent field method including only Coulomb potentials. In these calculations, we neglect the transverse Breit interaction and radiative corrections. These atomic orbitals are used to construct $(N+1)$-electron configuration state functions by performing configuration-interaction calculations as described above. Angular couplings of the atomic configuration state functions with the continuum orbitals and the numerical integrations of the continuum orbitals are performed with a modified version of the computer code RATR [20,21] that was originally developed to calculate autoionization amplitudes of Auger electrons. The continuum orbitals generated are orthogonalized to the atomic orbitals by Schmidt orthogonalization and are normalized to a given asymptotic flux. The calculations are iterated to self-consistency as discussed in Sec. II. Results based on this approach, calculating the elas-
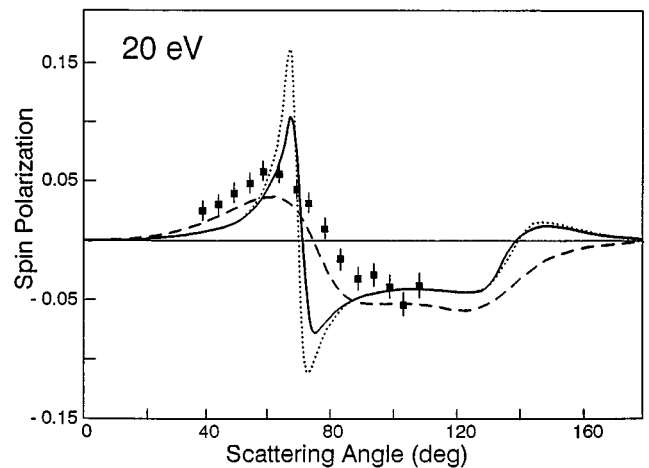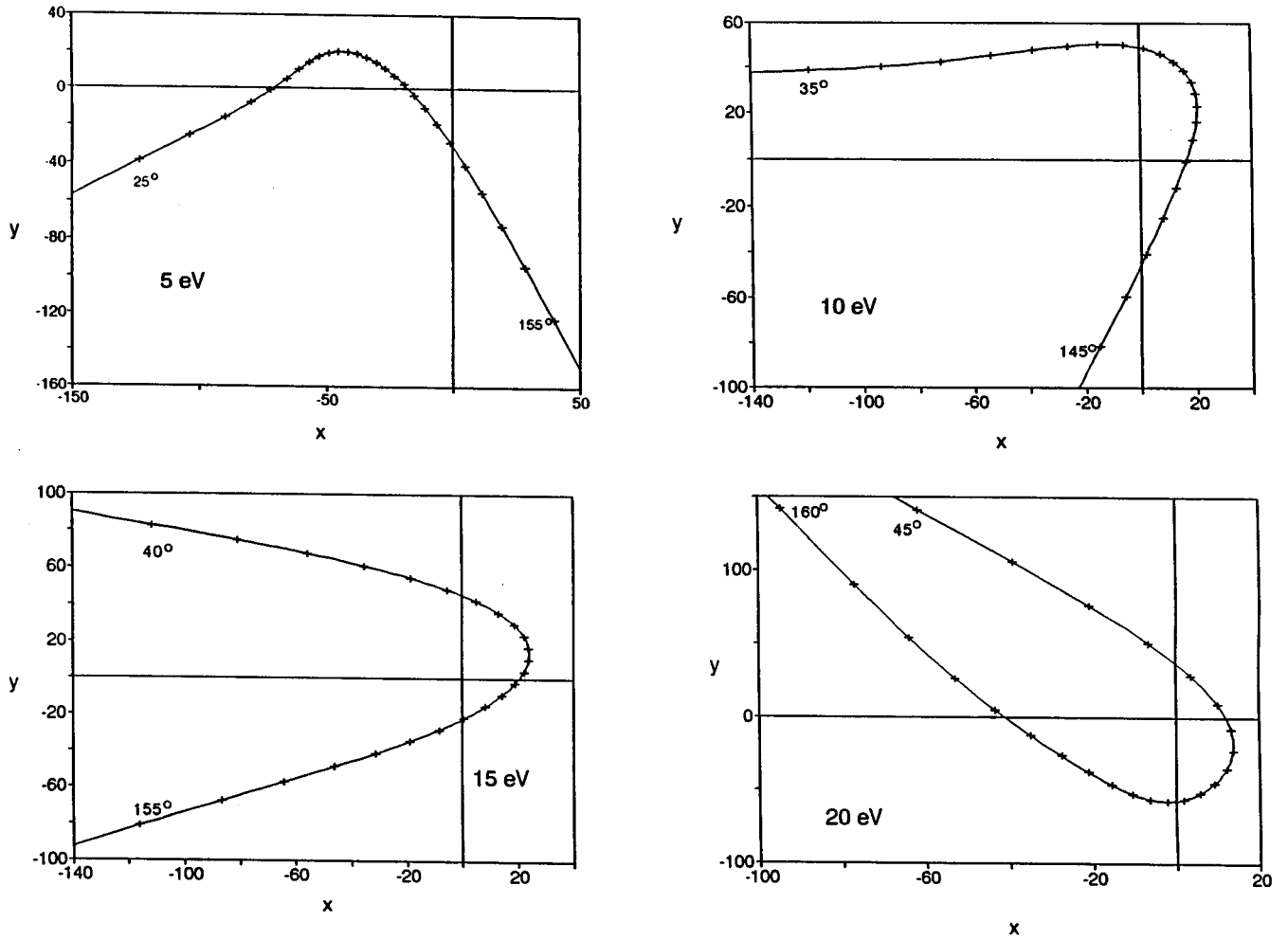
FIG. 4. As in Fig. 2, but at 20 eV.

FIG. 5. Polarization trajectories at 5, 10, 15, and 20 eV. Marks indicate scattering angles at $5°$ intervals. The trajectories move from the upper left with increasing scattering angle.

tic scattering of electrons by xenon atoms, are published elsewhere [4]. Relativistic phase shifts are calculated by comparing the numerical solutions of the Dirac-Hartree-Fock equations, Eqs. (6) and (7), to the analytical ones at large r where $rV(r) \rightarrow 0$:

$$\frac{P_\kappa(r)}{r} \sim j_l(kr)\cos\delta_l^\pm - n_l(kr)\sin\delta_l^\pm \; ,$$

where $k = \sqrt{2E + \alpha^2 E^2}$ is the momentum of the incident electron and $j_l(kr)$ and $n_l(kr)$ are the spherical Bessel and Neumann functions, respectively. We calculate phase shifts of the elastic channel for $l = 0, 1, \ldots, 6$. The sums in Eqs. (9) and (10) are extended to $l = 50$ by means of the approximate nonrelativistic Ali-Fraser [22] extrapolation formula.

IV. RESULTS AND DISCUSSION

The atomic ground-state wave function Φ_1 in Eq. (1) is calculated by a multiconfiguration wave function expansion over four relativistic configuration state functions coupled to form a $^1S_0$ term. These configurations are generated by single replacements of the two outermost orbitals $4s_{1/2}$ and $4p_{1/2,3/2}$ by the excited orbitals $4d_{3/2,5/2}$, $5s_{1/2}$, and $5p_{1/2,3/2}$. The calculated eigenenergy of the $^1S_0$ ground state

of the krypton atom is equal to $-2788.832\,5651$ hartrees.

The importance of target-atom polarization by the electric field of the scattering electron has been well documented [14]. It is found for electron scattering from krypton that only dipole polarization of the target atom is significant and that virtual excitations to the $5s$, $5p$, and $4d$ orbitals give the dominant contribution. It has been shown [24] that in the relativistic polarized-orbital approach the contribution of the distorted $4s_{1/2}$ and $4p_{1/2,3/2}$ orbitals to the static dipole polarizability exceeds 99.8%. In our calculations we take account of the dipole polarization of the $4s_{1/2}^2 4p_{1/2}^2 4p_{3/2}^4$ target krypton atom through the configuration-interaction procedure. The bound configuration state functions that account for the dipole polarization are $(N+1)$-electron determinants of $[Kr]$ $+5s_{1/2}$ and $[Kr]$ $+5p_{1/2,3/2}$ plus those configurations obtained by the single-electron replacements $4s_{1/2}, 4p_{1/2,3/2}$ $\rightarrow 4d_{3/2,5/2}, 5s_{1/2}, 5p_{1/2,3/2}$. The orbitals are taken from a relativistic multiconfiguration calculation for atomic krypton. With different angular-momenta couplings, 66 configuration state functions are generated in this way and included in the second sum of the scattering wave function, Eq. (4). For comparison, an approximation without target polarization can be calculated by omitting the second sum in Eq. (4).

Figs. 1–4 show our results for spin polarization at impact

energies of 5, 10, 15, and 20 eV, together with the experimental data of Beerlage *et al.* [10] and results of our previous relativistic calculations with a model-polarization potential [23]. The agreement with experiment is far better at the higher energy of 20 eV (Fig. 4), particularly if one takes into account the 8° angular resolution of the experimental data [10]. At a scattering energy of 10 eV (Fig. 2) both of our present results, with and without target polarization, fail to show the experimental peak around 100°. In this case our model-polarization calculations [23] are a bit closer to the experimental points, but the situation is still unsatisfactory. Additional results at 5 and 15 eV (Figs. 1 and 3), for which no experimental data are available, show differences between our different theoretical results.

The polarization trajectories calculated from the scattering amplitudes $f(\vartheta)$ and $g(\vartheta)$ for electron energies equal to 5, 10, 15, and 20 eV are presented in Fig. 5. Here, the information for all three spin-polarization parameters S, T, and U are displayed on single plots.

V. CONCLUSIONS

Relativistic multiconfiguration calculations have been presented for the elastic scattering of electrons by krypton for energies 5–20 eV. This approach has an advantage over model-polarization potential calculations in taking into account dynamic effects in a precise *ab initio* manner through the $(N+1)$-electron bound configurations. The method is parameter-free and can be applied not only to the obvious choice of noble gases as targets but to any other closed- or open-shell atom. In particular, it is suitable for heavy atoms, where relativistic effects play an important role. It should also be useful for calculations of inelastic cross sections.

We also present examples of spin-polarization trajectories. These are useful for presenting all spin-polarization information on a single plot. The concept of trajectories may be useful in showing the consistent agreement or disagreement between theoretical and experimental data.

[1] J. E. Sienkiewicz and W. E. Baylis, J. Phys. B **25**, 2081 (1992).

[2] R. P. McEachran and A. D. Stauffer, J. Phys. B **25**, 1527 (1992).

[3] R. Szmytkowski and J. E. Sienkiewicz, Phys. Rev. A **50**, 4007 (1994).

[4] J. E. Sienkiewicz, S. Fritzsche, and I. P. Grant, J. Phys. B **28**, L633 (1995).

[5] H. P. Saha, Phys. Rev. A **39**, 5048 (1989).

[6] H. P. Saha, Phys. Rev. A **43**, 4712 (1991).

[7] H. P. Saha, Bull. Am. Phys. Soc. **40**, 1294 (1995).

[8] R. P. McEachran and A. D. Stauffer, J. Phys. B **23**, 4605 (1990).

[9] D. J. R. Mimnagh, R. P. McEachran, and A. D. Stauffer, J. Phys. B **26**, 1727 (1993).

[10] M. J. M. Beerlage, Zhou Qing, and M. J. Van der Wiel, J. Phys. B **14**, 4627 (1981).

[11] I. P. Grant, Adv. Phys. **19**, 747 (1970).

[12] P. G. Burke, A. Hibbert, and W. D. Robb, J. Phys. B **4**, 150 (1971).

[13] A. Temkin, Phys. Rev. **107**, 1004 (1957).

[14] J. E. Sienkiewicz and W. E. Baylis, J. Phys. B **22**, 3733 (1989).

[15] J. Kessler, *Polarized Electrons*, 2nd ed. (Springer-Verlag, Berlin, 1985).

[16] W. E. Baylis and J. E. Sienkiewicz, J. Phys. B **28**, L549 (1995).

[17] F. A. Parpia, I. P. Grant, and C. Froese Fisher, GRASP2 (unpublished).

[18] I. P. Grant, B. McKenzie, P. Norrington, D. Mayers, and N. Pyper, Comput. Phys. Commun. **21**, 207 (1980).

[19] K. G. Dyall, I. P. Grant, C. T. Johnson, F. A. Parpia, and E. P. Plummer, Comput. Phys. Commun. **55**, 425 (1989).

[20] S. Fritzsche, Ph.D. thesis, University of Kassel, 1992 (unpublished).

[21] S. Fritzsche, Phys. Lett. A **180**, 262 (1993).

[22] M. A. Ali and P. A. Fraser, J. Phys. B **10**, 3091 (1977).

[23] J. E. Sienkiewicz and W. E. Baylis, J. Phys. B **24**, 1739 (1991).

[24] R. Szmytkowski, J. Phys. B **26**, 535 (1993).